

Bib DESY-Bibliothek
14. MRZ. 1966 ✓

DEUTSCHES ELEKTRONEN - SYNCHROTRON **DESY**

DESY 66/5
Februar 1966
Experimente

Measurement of Synchrotron Radiation in the X-Ray Region

by

G. Bathow and E. Freytag

Deutsches Elektronen-Synchrotron DESY, Hamburg, Germany

and

R. Haensel

Physikalisches Staatsinstitut, II. Institut für
Experimentalphysik der Universität Hamburg, Germany

(to be published in the Journal of Applied Physics)

2 HAMBURG 52 · NOTKESTIEG 1

MEASUREMENT OF SYNCHROTRON RADIATION IN THE X-RAY REGION

G. Bathow and E. Freytag
Deutsches Elektronen-Synchrotron DESY, Hamburg, Germany

and

R. Haensel †
Physikalisches Staatsinstitut, II. Institut für
Experimentalphysik der Universität Hamburg, Germany

Abstract

At the Deutsches Elektronen-Synchrotron DESY synchrotron radiation has been investigated by means of scintillation counters at electron energies between 4.0 and 6.3 GeV. Measurements were performed of the integrated radiation, the spectral distribution, the polarization and the angular dependence of them at photon energies between 15 and 300 keV. The results agree with theoretical calculations.

† Work supported by the Deutsche Forschungsgemeinschaft,
Bad Godesberg

I. Introduction

When passing through transverse magnetic field, relativistic electrons lose energy by emitting electromagnetic radiation. This radiation is generally known as synchrotron radiation, since it is particularly evident in electron synchrotrons. It has a continuous spectrum which - for accelerators with electron energies of some GeV - ranges from radio frequencies up into the X-ray region (a few hundred keV). The radiation is elliptically polarized and it is emitted symmetrically with respect to the electron orbital plane within an angle on the order m_0c^2/E_e . The radiation losses grow with the fourth power of the electron energy and largely determine the amount of power to be fed into the acceleration sections of electron synchrotrons or storage rings. For the latter, the synchrotron radiation will also give rise to vacuum deterioration by its continuous impact on the walls of the vacuum chamber¹⁾.

Knowledge of the characteristic features of synchrotron radiation is necessary for using it in certain experiments²⁾ as well as for interpreting some astrophysical data³⁾.

Experimental investigations of the spectrum, the angular distribution and the polarization of the synchrotron radiation were up to now mainly carried out in the visible region and the vacuum UV in accelerators with electron energies up to 1.2 GeV⁴⁻¹²⁾.

The present paper contains measurements carried out at the Deutsches Elektronen-Synchrotron DESY at electron energies between 4.0 and 6.3 GeV. It describes measurements of the total radiation emitted, its spectral distribution and polarization and the angular distribution, at photon energies between 15 and 300 keV.

II. Theoretical Considerations

The theory of the synchrotron radiation has been treated in several papers¹³⁻²⁰). In the following we are referring to Schwinger¹³). For any possible angle ψ (the angle between the direction of emission and the orbital plane) one obtains for the radiation intensity I at an electron E_e and a frequency ω of the emitted photons

$$\frac{\partial^2 I(\psi, \omega, E_e)}{\partial \psi \partial \omega} = \frac{3}{4\pi^2} \frac{e^2}{R} \left(\frac{\omega}{\omega_c}\right)^2 \gamma^2 (1 + \gamma^2 \psi^2)^2 \left[K_{2/3}^2(\xi) + \frac{\gamma^2 \psi^2}{1 + \gamma^2 \psi^2} K_{1/3}^2(\xi) \right] \quad (1)$$

$$\text{where } \xi = \frac{1}{2} \frac{\omega}{\omega_c} (1 + \gamma^2 \psi^2)^{3/2} \quad (1a)$$

$$\text{and } \omega_c = \frac{3}{2} \frac{c}{R} \gamma^3 \quad (1b)$$

$$\text{and } \gamma = E_e / m_0 c^2 \quad (1c)$$

R is the radius of the electron orbit in the magnet, e is the elementary charge, $K_{1/3}$ and $K_{2/3}$ are modified Bessel functions of the second kind.

For comparison with the measurements Eq. (1) is converted into photons/(sec.eV.rad)

$$\frac{\partial^3 N(\psi, E_{ph}, E_e)}{\partial \psi \partial E_{ph} \partial t} = 1.602 \cdot 10^{12} \frac{e^2}{2\pi^2 c R} \frac{E_{ph}}{E_c} \gamma^{-1} (1 + \gamma^2 \psi^2)^2 \left[K_{2/3}^2(\xi) + \frac{\gamma^2 \psi^2}{1 + \gamma^2 \psi^2} K_{1/3}^2(\xi) \right] \quad (2)$$

$$\text{where } \xi = \frac{1}{2} \frac{E_{ph}}{E_c} (1 + \gamma^2 \psi^2)^{3/2} \quad (2a)$$

$$\text{and } E_c = (3hc/2R) \cdot \gamma^3 \quad (2b)$$

All constants are given in cgs units.

The two terms in the last parentheses of Eqs. (1) and (2) represent the contributions of the two directions of polarization. The first one describes the contribution in which the oscillation of the E-vector is parallel to the synchrotron

plane, and the second one represents the perpendicular component. Integrating Eq. (2) over the angle ψ one gets in photons/(sec·eV)

$$\frac{\partial^2 N(E_{ph}, E_e)}{\partial E_{ph} \partial t} = 1,602 \cdot 10^{-12} \frac{e^2}{\sqrt{3} \pi c R^2} \gamma^{-2} \int_{E_{ph}/E_{ph,c}}^{\infty} K_{5/3}(\eta) d\eta \quad (3)$$

Eqs. (1) to (3) are valid for a constant energy E_e . In accelerators, however, E_e is a function of time. For DESY we have $E_e = E_{max} \sin^2(\pi t/2T)$, where T is the time of acceleration. After integration over t one can derive from Eq. (1) the intensity in the spectrum of the synchrotron radiation as a function of the angle ψ and the frequency ω , integrated over the time of acceleration.

$$\frac{\partial^2 \bar{I}(\psi, \omega, E_{max})}{\partial \psi \partial \omega} = \frac{9 e^2 \gamma^2}{\pi^3 R} \left(\frac{\omega}{\omega_c} \right)^2 L(\psi, \omega, E_{max}) \quad (4)$$

The function $L(\psi, \omega, E_{max})$ can be taken from Ref. 21. After integrating over ψ and ω , one gets for the total intensity of the emitted radiation, averaged over the time of acceleration

$$\bar{I}(E_{max}) = (35/192) (e^2 c / R^2) \gamma_{max}^4 \quad (5)$$

This term will subsequently be referred to as the total radiation.

III. General Conditions for the Experiment

The radius R of the electron orbit in the DESY synchrotron magnets is 31,70 m, the mean radius of the machine is 50.42 m, because there are straight sections between the magnets. The orbital frequency of the electrons in the synchrotron therefore is 946 kHz.

The synchrotron radiation used in our experiment passes from the center of a deflecting magnet through a tangential beam

tube into the experimental area. The beam tube is 35 m long, has a diameter of 65 mm and is directly connected to the accelerator vacuum. It subtends an angle of ± 0.75 mrad, which is amply sufficient for the measurements described in this paper. According to Eq. (1), the intensity of radiation for this angle is smaller than 10^{-3} of the maximum value at $E_e > 3 \text{ GeV}^{22}$).

IV. Measurement of the Total Radiation

The total radiation was measured with a totally absorbing lead glass scintillator. The scintillation output is proportional to the intensity independent of the photon energy²³). An absolute calibration was carried out with a 30 keV electron beam.

The experimental set-up is shown in Fig. 1. In order to eliminate the visible part of the synchrotron radiation, which would overlap the scintillation light and contaminate the measurement, an aluminum layer of 1μ thickness was evaporated onto the lead glass. The absorption of this coating limits the spectral range to $E_{ph} > 1.5 \text{ keV}$. Additional aluminum filters could optionally be put in front of the lead glass scintillator in the beam tube. They were designed to transmit approx. 10 % of the total radiation at electron energies of 4.0, 5.0 and 6.0 GeV respectively on the basis of the predicted spectral curve. The thicknesses of the filters were 0.1, 0.8 and 3.5 mm respectively.

Fig. 2 shows the results of the measurements. For comparison it includes the predicted curve of the total radiation as a function of the final electron energy E_{max} (curve No. 1). Curve No. 2 takes into consideration the absorption of the aluminum coating. Curve No. 3 shows the measured points when the filters were inserted. The error bars, shown in Fig. 2 do not include a possible uncertainty in the calibration of the circulating electron beam current.

We have also measured the radiation dose with an air ionization chamber for an electron energy of 6 GeV and for a circulating electron current of about 1 mA. In these measurements the synchrotron radiation had to penetrate a vacuum tight 0.2 mm Be window, which also served as an electrode of the measuring chamber. The useful chamber volume was 30 mm³, and the tension on the chamber amounted to 1.2 keV. The radiation dose rate, as measured 30 m from the source, was 10⁴ r/sec. Since the radiation was pulsed with the repetition frequency of the synchrotron (50 Hz) and it is mainly produced during the last msec of the acceleration, the pulse dose rate amounts to approx. 2·10⁵ r/sec. The calculated spectral maximum radiation dose rate lies at about 2 keV.

V. Experimental Arrangement for the Measurements of the Spectral Distribution and Polarization

For measurements with the direct beam, thick absorbers must be employed because of the high intensity of the synchrotron radiation in the low energy region. For photon energies above 100 keV the attenuation is low and the original spectral can be computed from the measured data. However, these corrections are not accurate below 100 keV. In this region the intensity was reduced by 90° Compton scattering. The resulting change in the photon energy and the relative dependence of the Compton cross section on the energy were taken into consideration by introducing the Klein-Nishina formula

$$d\sigma = \frac{\tau_0^2}{2} d\Omega \left(\frac{E'_{ph}}{E_{ph}} \right)^2 \left(\frac{E_{ph}}{E'_{ph}} + \frac{E'_{ph}}{E_{ph}} - 2 \sin^2 \vartheta \cos^2 \eta \right) \quad (6)$$

$$\text{and} \quad E'_{ph} = E_{ph} / \left(1 + (E_{ph} / m_0 c^2)(1 - \cos \vartheta) \right) \quad (6a)$$

E'_{ph} is the energy of the scattered photons, ϑ is the scattering angle, η is the angle between the electric vector and the scattering plane, r_0 is the classical electron radius.

The synchrotron radiation leaves the beam tube through the 0.2 mm Be window (see Fig. 3), passes a hole in the lead shielding wall, and reaches the target through a perpendicular lead slit, which serves as a collimator. A 2 mm polyethylene target was used, which proved suitable as scattering material because of its low atomic number. The beam was shielded by lead tubes in order to avoid additional air scattering at angles other than 90° .

Above and beside the target two scintillation counters were mounted at equal distances (53 AVP photomultipliers with NaJ(Tl)-crystals). They covered both parts of the polarization (see VII), the sum of which gives the spectrum of the synchrotron radiation (see VI). A third scintillation counter served as a monitor, when it was mounted above the beam, or for direct measurement of the spectrum in the unscattered beam, when put in the direction of the beam with absorbers in front of it. The pulses coming from the scintillation counters were stored in a 256 channel pulse-height analyzer (RIDL Nano-lyzer) simultaneously in three quadrants.

By trigger pulses coming from the synchrotron, an interval of 0.5 msec at the end of the acceleration was selected for the measurement. The uncertainty in energy owing to the gate width is smaller than 2 %.

The energy calibration was done with the gamma lines of a Ba^{133} source (31 keV, 79 keV and 358 keV).

VI. Measurements of the Spectral Distribution

The spectral distribution integrated over the angle ψ is described by Eq. (3). The function $\int_x^{\infty} K_{5/3}(z) dz$ included therein was computed on an IBM 7044, and is plotted in Fig. 4. It shows that the photon density varies by about a factor of 12 per 10 keV photon energy at an electron energy of 4 GeV.

This extreme slope makes even small pile-up effects in the crystal sensibly affect the spectrum. The counting rate therefore had to be kept down to avoid distortions of the spectrum.

When measuring spectra with such a steep slope one has to evaluate the energy resolution of the apparatus rather carefully, since finite resolution flattens the spectrum. Measurements were made with the Ba¹³³ calibration spectrum (FWHS approx. 33 % at 31 keV and approx. 20 % at 79 keV). The unfolding of the measurements was done on an IBM 7044 permitting the deduction of the real slope.

Fig. 5 shows some examples of the results for several electron energies. At 6.3 GeV the measurements above 120 keV photon energy were made in the direct beam with 20 mm Fe and 139 mm Al absorbers. The other points were obtained with the scattered radiation. When comparing the observed slope with the predicted values obtained from Fig. 4, agreement was found within an electron energy deviation of 3 %. Since the beam current of the synchrotron is only known to an accuracy of ± 50 %, the agreement with the predicted curves contains the same uncertainty, which is included in the error bar of Fig. 5.

VII. Measurements of the Polarization

In Eq. (2) the terms in the last parenthesis describe the angular dependence of the two parts of the polarization. After numerical integration over the angle ψ one obtains the polarization values P , shown in Fig. 6, which depend on the photon and electron energies. The polarization ratio P is defined as

$$P = \frac{(I_{\parallel} - I_{\perp})}{(I_{\parallel} + I_{\perp})} \quad (7)$$

Measurements of the polarization were made with the set-up described in V by means of the Compton scattering. The upper scintillation counter detects that part of the radiation which is polarized parallel to the synchrotron plane, while the lateral

counter detects the part which is polarized in the perpendicular direction. This holds rigidly only for the limiting case, where $E_{ph} = E_{ph}'$; for higher photon energies corrections according to the Klein-Nishina formula (6) have to be taken into consideration. Fig. 6 shows the measurements for four different electron energies. Errors are due to the low counting rate at low electron energies and to background at high electron energies. Both effects result in a reduction of the polarization coefficient.

In order to obtain measurements of both polarization components under exactly the same conditions, it was necessary to store them simultaneously in the multichannel analyzer. The different characteristics of the scintillation counters were taken into consideration by interchanging the counters and by the use of the monitor.

VIII. Angular Distribution

The synchrotron radiation is emitted in an angular interval on the order γ^{-1} with respect to the synchrotron plane. This holds true for the total radiation. For high photon energies the collimation becomes stronger, while for lower photon energies it is weaker than the above mean value. Thus the angular range is of the order 1 mrad for photons in the visible spectral region, while it is of the order 10^{-2} mrad in the X-ray region. This distribution shows the effects of a superposition of the true angular distribution and of the influence of the finite height of the synchrotron beam (approx. 2 mm). For the measurement of the angular distribution the vertical slit in Fig. 3 was substituted by a horizontal slit of 1 mm height which could be moved vertically.

The following figures illustrate the differences between the ideal case of an infinitely thin electron beam and the values resulting from the finite beam height. For calculations, the

finite beam height was introduced by the assumption of a circular cross section of the electron beam. Varying the radius of this beam in steps of 0.5 mm, the best fit for all measurements of the spectral distribution and polarization was obtained for $r = 2.0$ mm. The difference between this effective beam diameter of 4 mm and the observed beam height of 2 mm can be explained by the divergence of the electron beam.

Fig. 7 shows the angular distribution of the intensity for several photon energies. Only relative values are plotted and the intensity for $\psi = 0$ is normalized to 100 %. The decrease of the angle with increasing photon energy can be seen clearly. Besides of the theoretical values for the infinitely thin beam ($r = 0$ mm), the calculated curves for $r = 2$ mm are also shown. The influence of the finite beam height is most significant at high photon energies.

Two examples of the measured values for the angular dependent spectral distribution are shown in Fig. 8. It contains the predicted curves according to Eq. (2) (for $r = 0$ mm) as well as those for $r = 2$ mm together with the measured points. The spectral distribution becomes steeper with increasing angle owing to the particular angular distribution for different photon energies as discussed above.

Fig. 9 shows the dependence of the polarization on the angle ψ for an electron energy of 5.2 GeV. The assumption of a beam radius of $r = 2.0$ mm explains also the observed splitting for different photon energies. For comparison the predicted distribution for an infinitely thin beam is presented which is approximately valid for all photon energies investigated.

IX. Conclusions

At electron energies of some GeV, the largest part of the synchrotron radiation lies in the X-ray region. The measurements reported in the present paper permit us to investigate

with one single method

- a) the total radiation of which about 90 % are covered,
- b) the spectrum in an energy range from 15 to 300 keV,
- c) the polarization in an energy range from 15 to 300 keV,

as a function of the electron energy between 3.0 and 6.3 GeV. Within the accuracy of measurement agreement was found with the theory of the synchrotron radiation up to maximum photon energies.

Acknowledgements

The authors are indebted to the Deutsche Forschungsgemeinschaft for a grant, which made possible the synchrotron radiation research program. They also wish to thank Prof. W. Jentschke, Prof. P. Stähelin and Prof. M.W. Teucher for their continuous support of the work during preparation and execution of the measurements, as well as Dr. O. Beer for initiating this investigation and Dr. G. Buschhorn for discussions. Finally their sincere thanks go to the operating staff for running the machine.

Figure Captions

- Fig. 1 Experimental arrangement for the measurements of the total radiation.
- Fig. 2 Power (mW/mA·cm) radiated per mA circulating beam current into a vertical slit of 1 cm width at a distance of 35 m averaged over the full acceleration time as a function of the final electron energy (GeV).
Curve 1 - Theoretical values without filter,
Curve 2 - 1 μ Al filter taken into account, O measured values,
Curve 3 - With Al filters absorbing 90 %, + measured values.
- Fig. 3 Experimental arrangement for the measurement of the spectral distribution and polarization.
- Fig. 4 Universal curve for the spectral distribution. According to Eq. 2b for DESY $E_c(\text{keV}) = 7.0 \cdot 10^{-2} E_e^3(\text{GeV})$.
- Fig. 5 Photon flux (photons/sec·eV) radiated per electron into a vertical slit of 1 cm width at a distance of 37.6 m as a function of photon energy for several electron energies. The lines represent the theoretical values.
- Fig. 6 Polarization of the synchrotron radiation as a function of the electron and photon energy. The lines represent the theoretical values.
- Fig. 7 Angular distribution of relative intensity for several photon energies and 5.2 GeV electron energy. The intensity for $\psi = 0$ is normalized to 100 %. Curves represent the theoretical values for $r = 0$ mm and $r = 2$ mm.
- Fig. 8 Relative photon flux (photons/(eV·sec)) as a function of photon energy for two angles with respect to the synchrotron plane. Electron energy is 5.2 GeV. The lines represent the theoretical values for $r = 0$ mm and $r = 2$ mm.
- Fig. 9 Angular distribution of the polarization values for several photon energies. The electron energy is 5.2 GeV. The curves represent the theoretical values for $r = 2$ mm, the dotted line gives the values for $r = 0$ mm.

References

1. G.E. Fischer and R.A. Mack, CEAL 1017
2. R.P. Madden and K. Codling, Phys.Rev.Lett. 10, 516 (1963)
K. Codling and R.P. Madden, Phys.Rev.Lett. 12, 106 (1964)
R.P. Madden and K. Codling, J.Opt.Soc.Am. 54, 268 (1964)
3. M.M. Shapiro, Science 135, 175 (1962)
4. D.H. Tomboulain and P.L. Hartman, Phys.Rev. 102, 1423 (1956)
5. I.M. Ado and P.A. Cherenkov, Soviet Phys.Doklady 1, 517 (1956)
6. F.A. Korolev, V.S. Markov, E.M. Akimov and O.F. Kulikov, Dokl.Akad.Nauk.SSSR 110, 542 (1956)
7. F.A. Korolev and O.F. Kulikov, Opt. Spectry 8, 1 (1960)
8. F.A. Korolev, O.F. Kulikov and A.S. Yarov, Soviet Phys.-JETP 43, 1653 (1953)
9. K. Codling and R.P. Madden, J. App.Phys. 36, 380 (1965)
10. P. Joos, Phys.Rev.Letters 4, 558 (1960)
11. F.R. Elder, R.V. Langmuir and Pollock, Phys.Rev. 74, 52 (1948)
12. Y. Cauchois, Ch. Bonnelle and G. Missoni, Compt.Rend. 257, 409 (1963)
Y. Cauchois, Ch. Bonnelle and G. Missoni, Compt.Rend. 257, 1242 (1963)
13. J. Schwinger, Phys.Rev. 75, 1912 (1949)
14. K.C. Westfold, Astrophys.J. 130, 241 (1959)
15. D.D. Ivanenko and I. Pomeranchuk, Phys.Rev. 65, 343 (1943)
16. D.D. Ivanenko and A.B. Sokolov, Dokl.Akad.SSR 59, 1551 (1948)
17. H. Olsen, Kgl.Norske Videnskab.Selskab.Skrifter Nr.5 (1952)
- 18) H. Olsen and H. Wergeland, Phys.Rev. 86, 123 (1952)
19. H. Olsen, NBS-Report 7016 (1960)
20. D.H. Tomboulain, Dep. of Phys.Cornell Univ.Techn.Rep. No. 1 (1960)
21. G. Ripken, DESY-Notiz A.2.90
22. R. Haensel, DESY-Notiz A.2.101
23. H. Hermann, G. Bathow, H. Oeser and J. Broser, Fortschr. Röntgenstr.u.Nuklearmed. 88, 458 (1958)

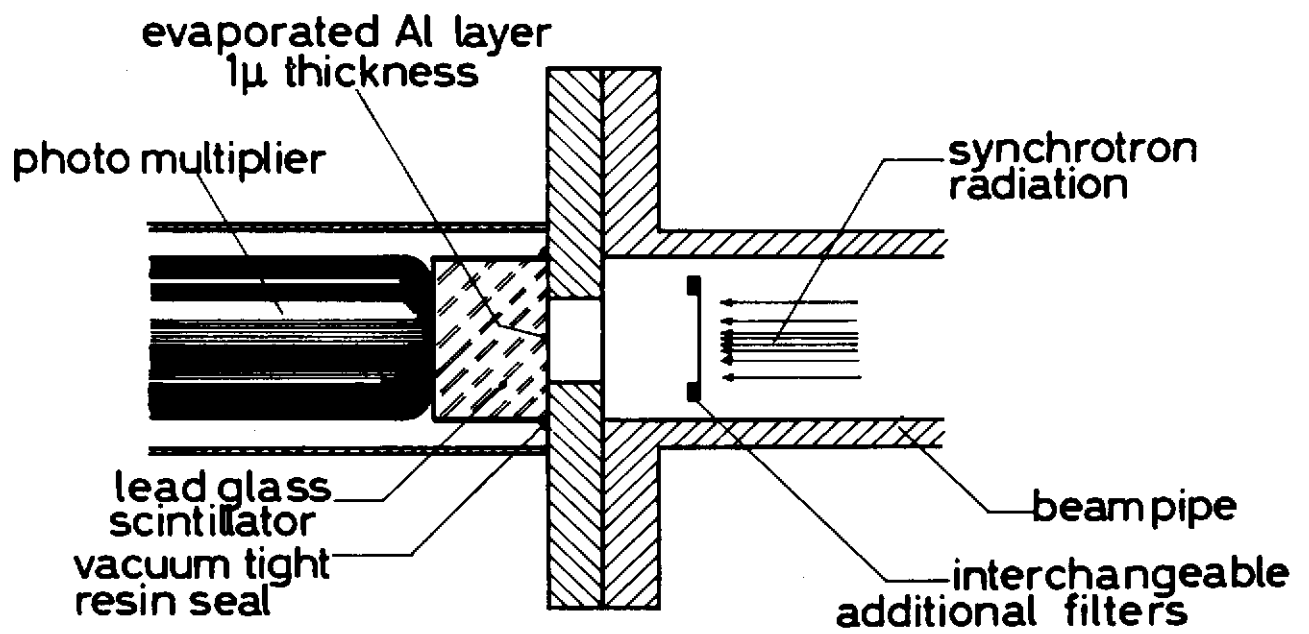


fig.1

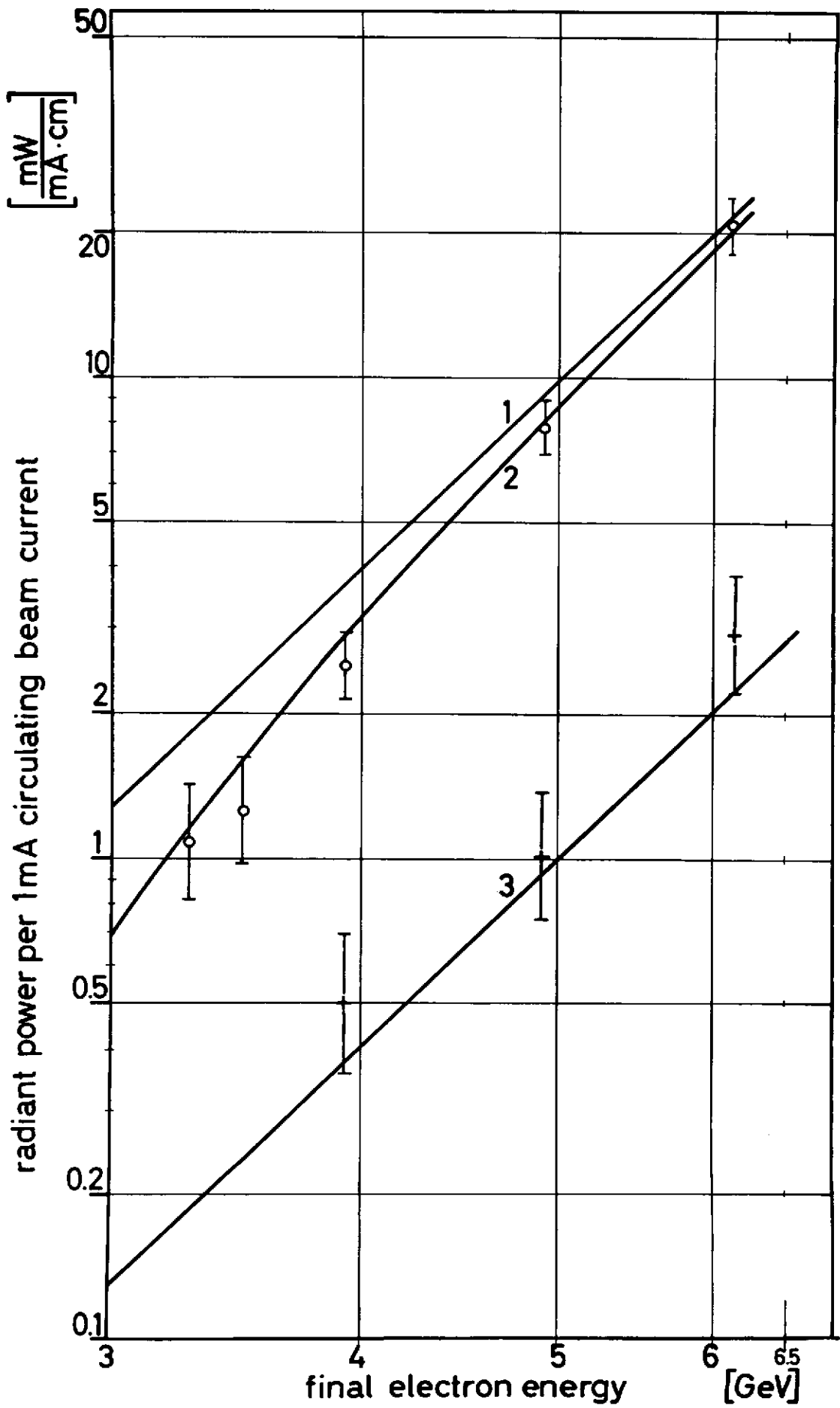


fig.2

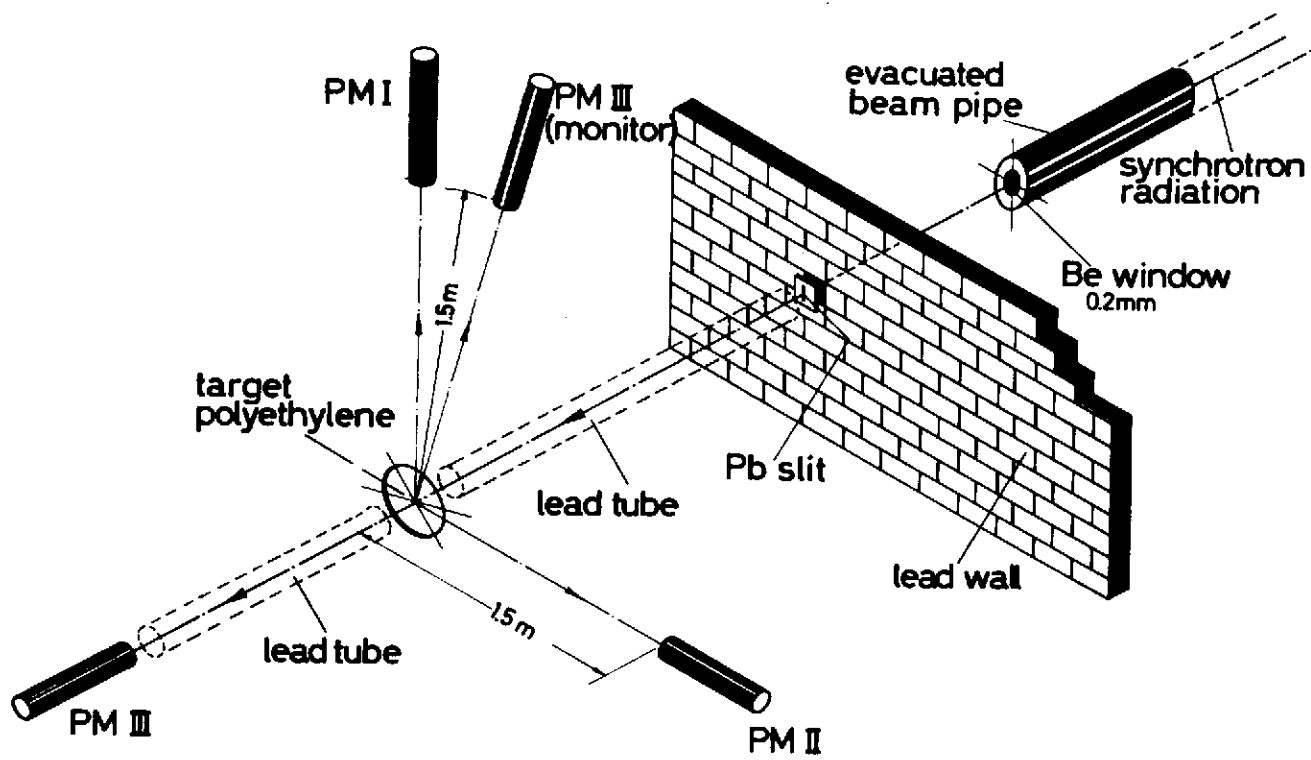


fig.3

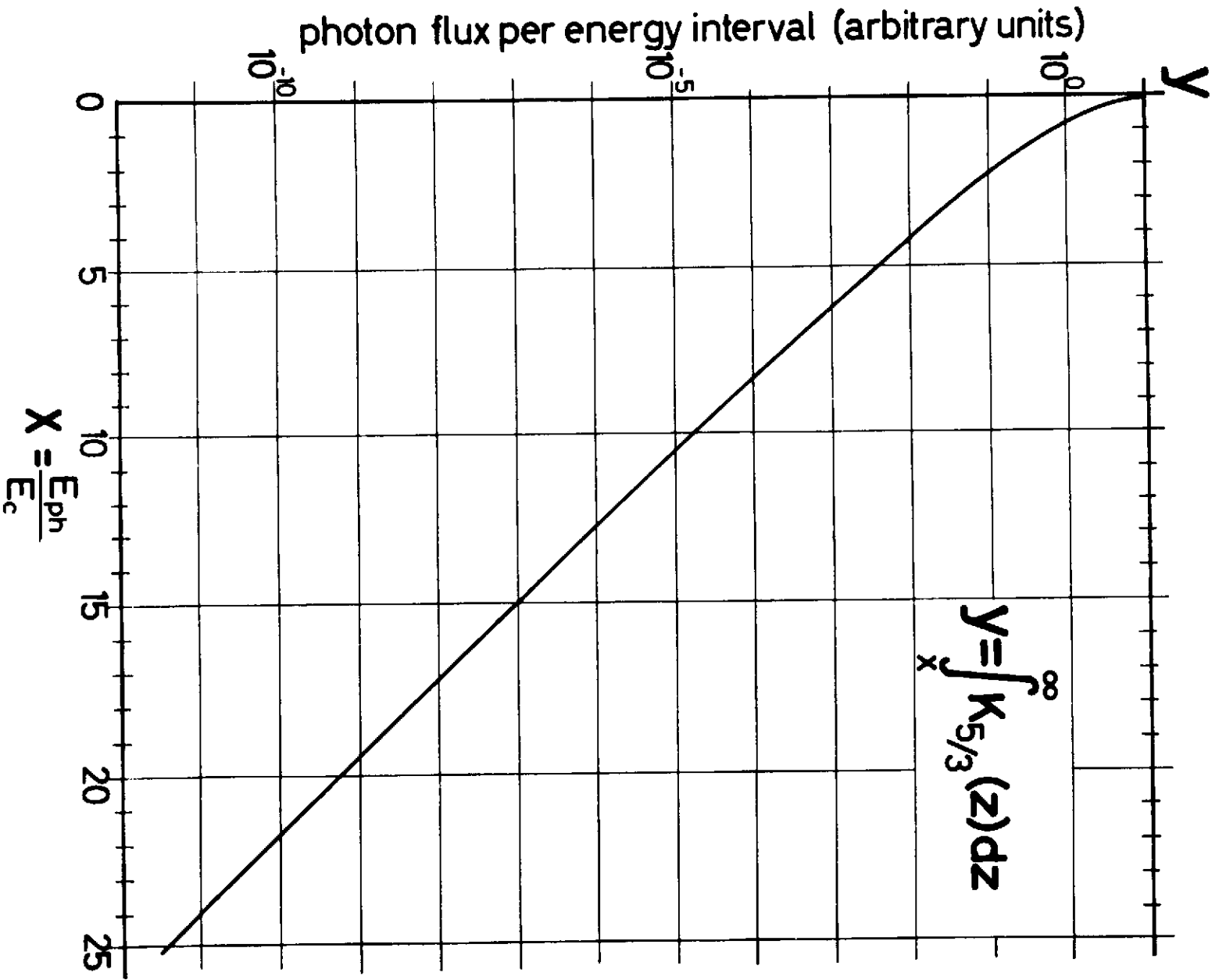


fig. 4

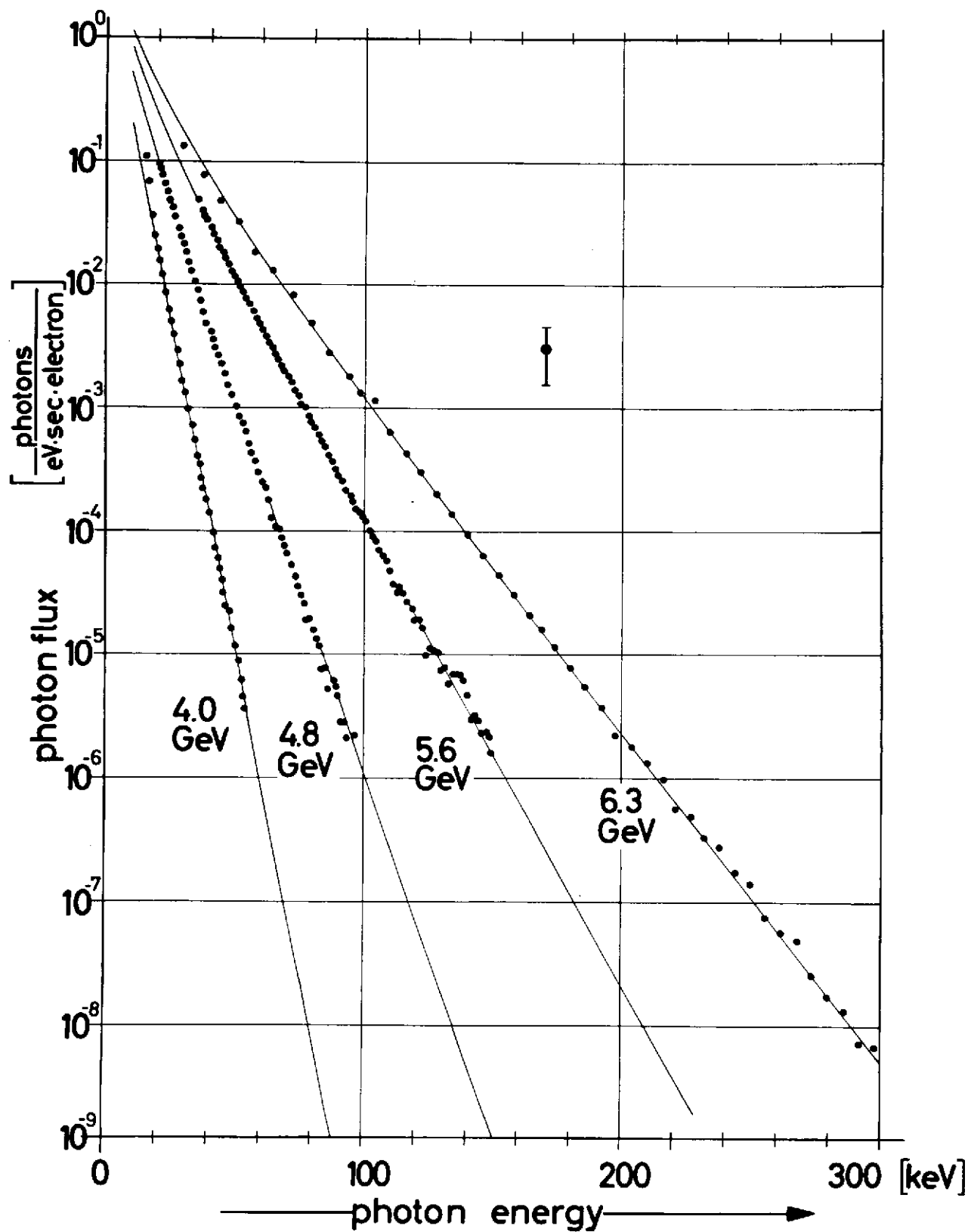


fig.5

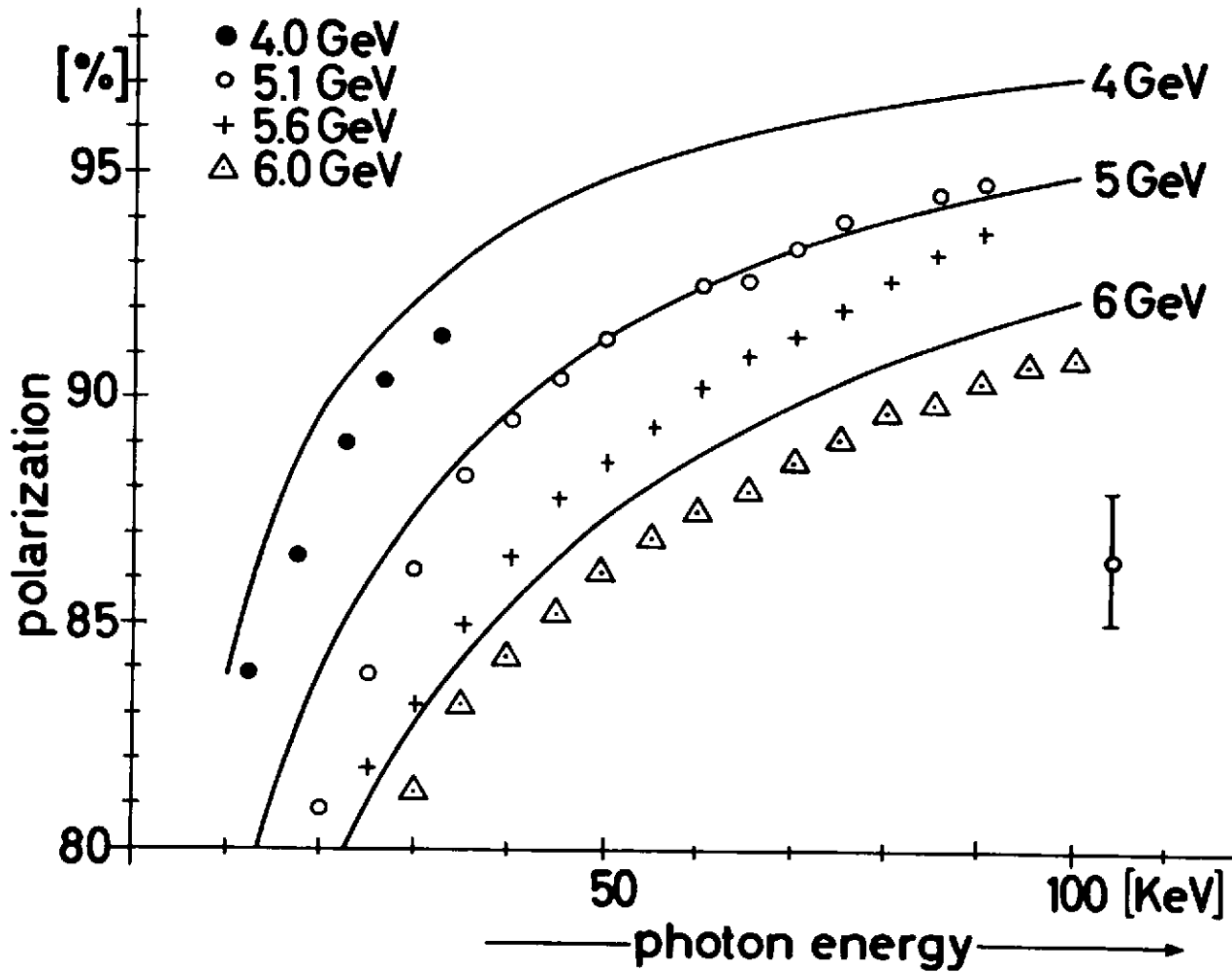


fig.6

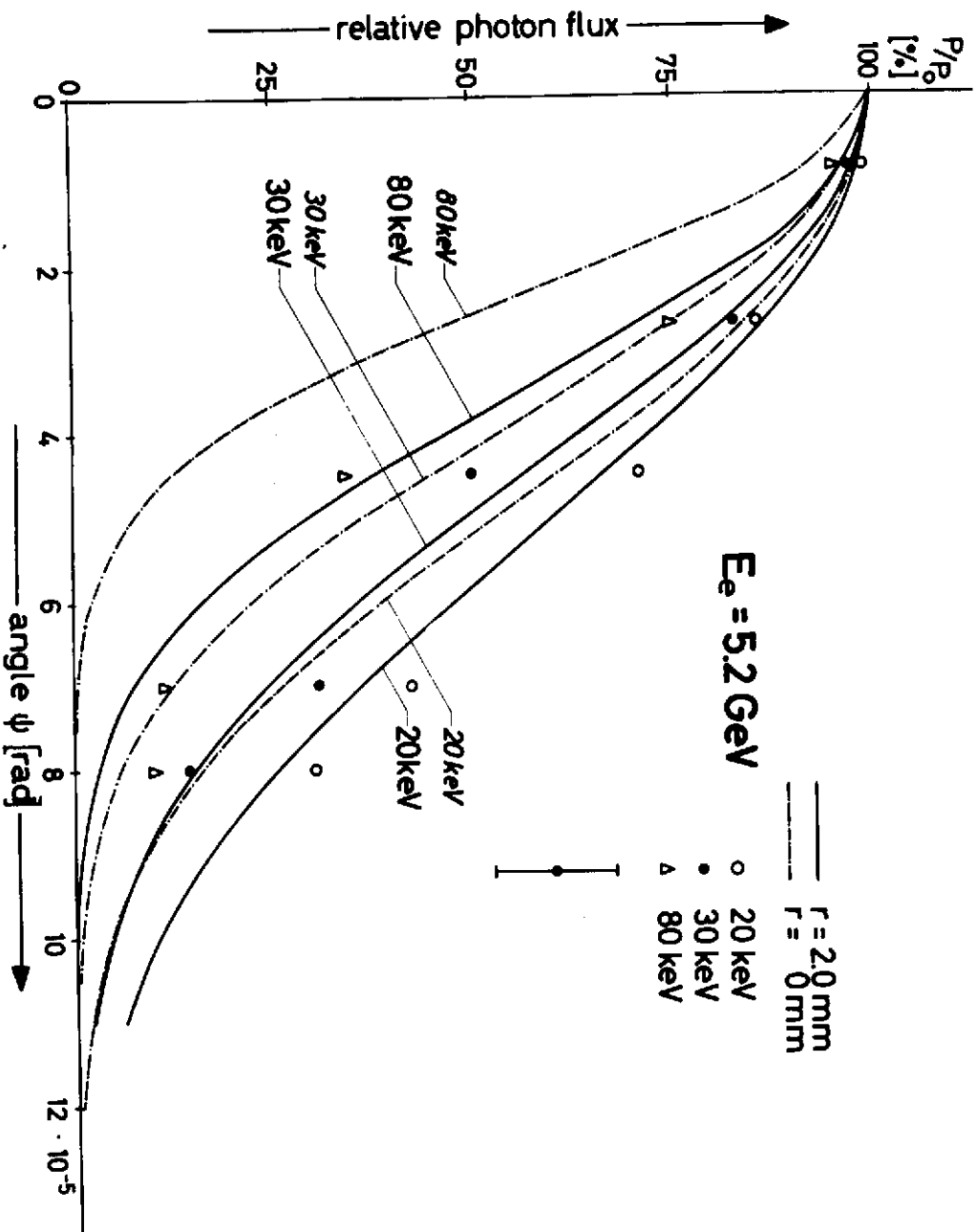


fig. 7

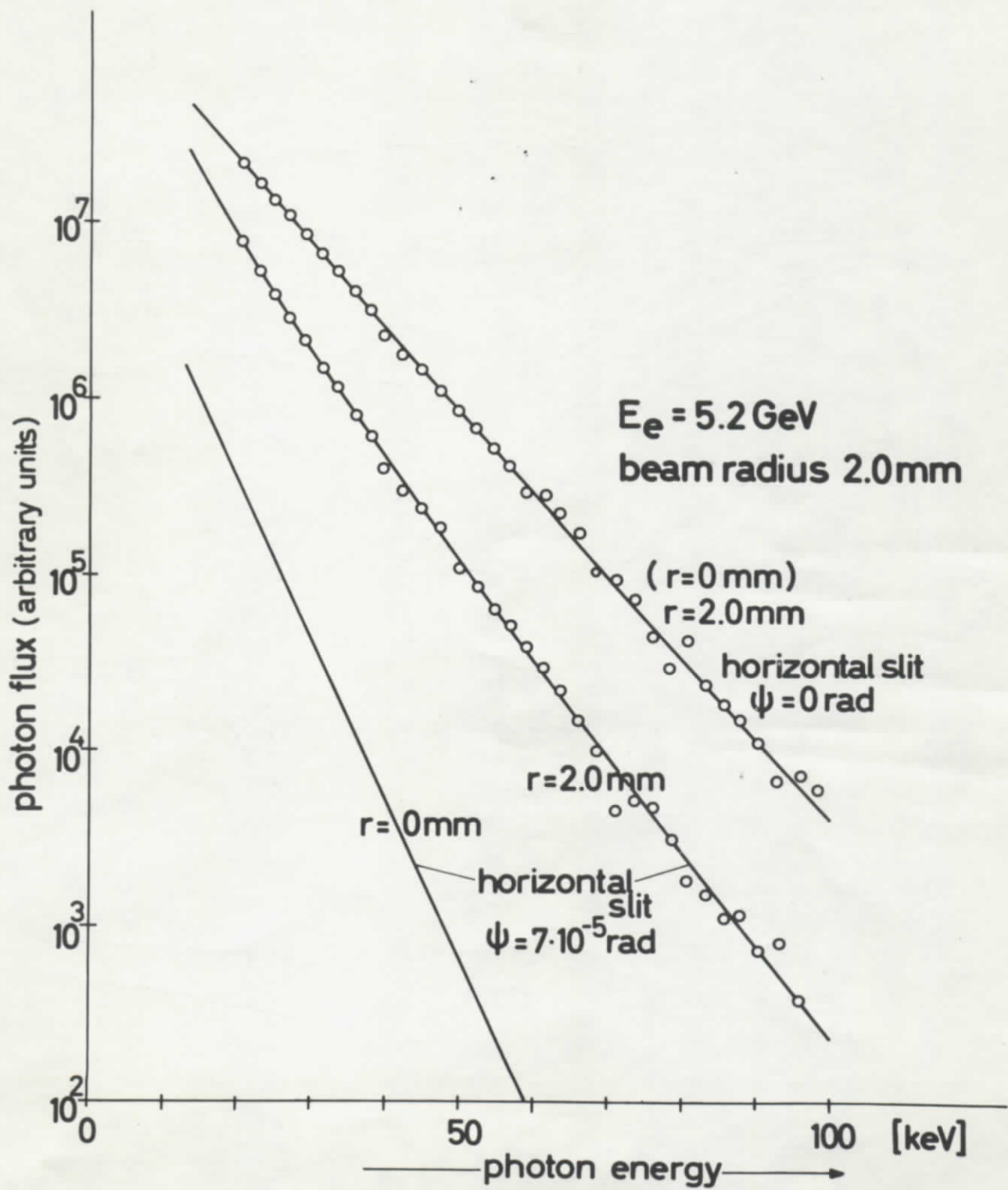


fig.8

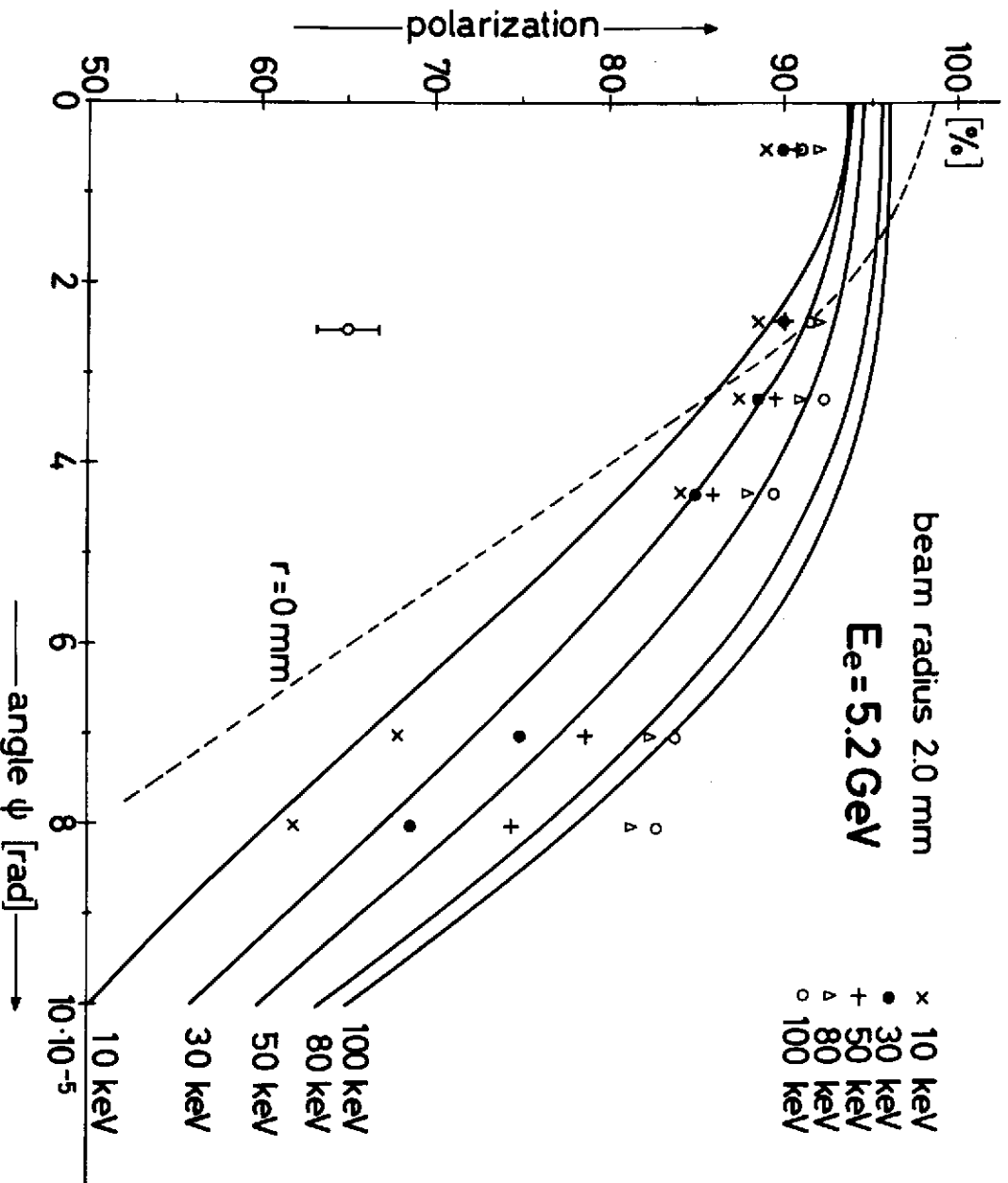


fig. 9